POLITECNICO
MILANO 1863

Automation and Control Engineering

CONSTRAINED NUMERICAL OPTIMIZATION FOR ESTIMATION AND CONTROL

OPTIMAL CONTROL OF A VARIABLE-PITCH WIND TURBINE

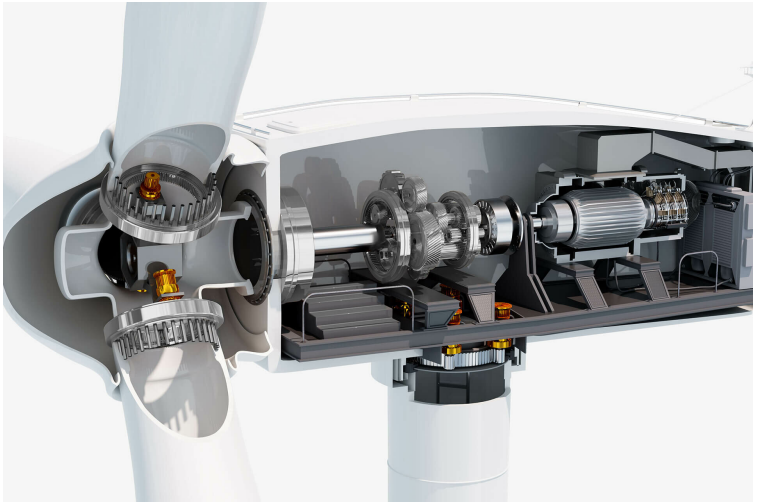

Authors:
Alessandro Lupatini
Diego Malusardi
Mar Puchades Ibáñez
Marco Rositani

Contents

1 Introduction

Since ancient times, the power of the wind has been exploited in various ways, predominantly for milling grain and pumping water. However, the dawn of the industrial age saw a shift from wind energy to fossil fuels, with windmills largely being used to pump water for farming purposes. The oil crisis in the early 1970s sparked a transformation in wind technology. Driven by the surge in oil prices, numerous countries started extensive research and development programs for wind energy. This led to the advent of new materials and contemporary turbine designs, marking the beginning of large-scale electricity generation from wind. Over the past few decades, growing environmental concerns and the trend towards diversifying the energy market have further amplified interest in harnessing wind energy [1].

Nowadays, wind energy stands out as the fastest-growing renewable energy source. As young individuals, we are acutely aware of the critical need to enhance renewable energy technologies, particularly in the realm of wind energy, which has become indispensable in today's world. Moreover, the importance of wind power is exponentially increasing, evidenced by the expansion of wind turbine installations across Europe. We believe this represents an opportune moment to delve into the study of wind turbine control [1].

Additionally, we recognize that active control has a direct impact on the cost efficiency of wind energy and the development of high-performance and reliable controllers is paramount for enhancing the competitiveness of wind technology.

Thus, the focus of this project is to design a suitable control strategy to ensure energy cost efficiency and the reliability of wind turbines.

In this report we will address what we have done in our project. First of all, in Ch. 2 we describe what are the main characteristic of a wind turbine. From that description, a mathematical model is derived to study its behaviour. After that we have a model of the system, in Ch. 3 we specify the control problem we need to solve, focusing on the control objectives and analyzing the possible solutions. The chosen solution implies the resolution of an optimization problem, so in Ch. 4 we address the way it can be solved. Finally, in Ch. 5 we illustrate the simulations and results that we achieved with our strategy, making comparisons between different kind of solutions. We added also a Ch. 6. in which all the mathematical parameters values are grouped.

2 System

2.1 System description

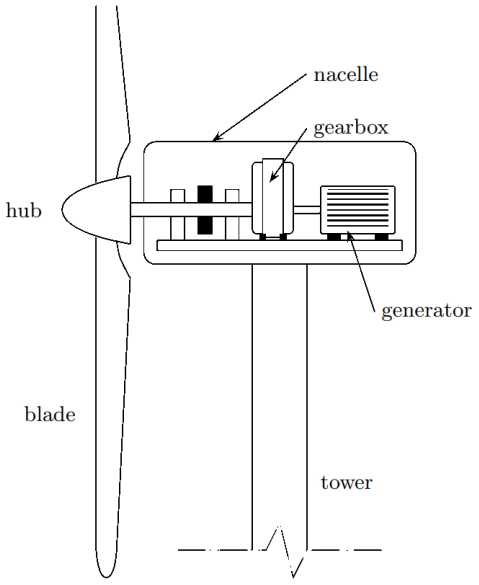

Figure 1: WECS with horizontal-axis wind turbine

The main components of a WECS are:

- The **blades** are the aerodynamic manifolds that allow to transform the power generated by the wind, into mechanical power trough their rotation.
- The **rotor** comprises the hub that links the blades to the transmission and the pitch servos, which are placed inside the hub, that rotate the blades around their longitudinal axes.
- The **transmission system** transmits the mechanical power captured by the rotor to the electric machine. It comprises the low- and high-speed shafts, the gearbox and the brakes. The gearbox increases the rotor speed to values more suitable for driving the generator.
- The **electric generator** is the device that converts mechanical power into electricity. Its electric terminals are connected to the utility network.
- The **tower** is the structure that supports the nacelle and all the elements described before. It also allows the blades to be positioned in an high place, where the wind is more powerful.

A model for the entire Wind Energy Conversion System (WECS) can be structured as several interconnected subsystem models as it is shown in figure 2. The aerodynamic subsystem describes the transformation of the wind speed profile into forces on the blades that

originate the rotational movement. The mechanical subsystem can be divided into two functional blocks, i.e., the drive-train and the support structure. The drive-train transfers the aerodynamic torque on the blades to the generator shaft. It encompasses the rotor, the transmission and the mechanical parts of the generator. The structure comprised by the tower and foundations supports the thrust force. The electrical subsystem describes the conversion of mechanical power at the generator shaft into electricity. Finally, there is the actuator subsystem that models the pitch servo behaviour[1].
In particular the model will be based on a 5-MW variable-pitch wind turbine with horizontal-axis and three blades [2].

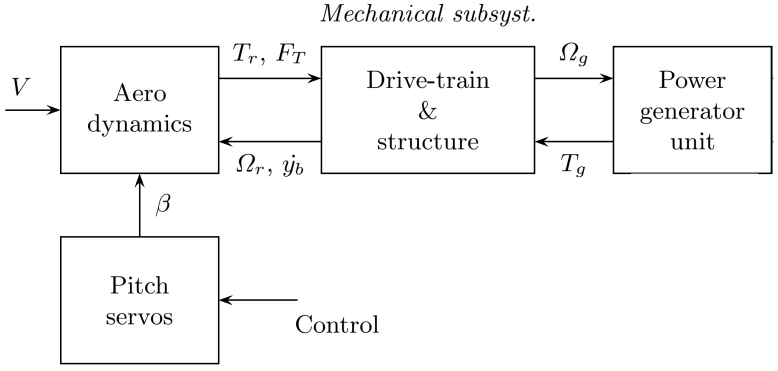

Figure 2: Subsystem-level block diagram of a variable-pitch WECS

2.2 Assumptions

Several assumptions were made to derive a control-oriented model.

- Mechanical:
  - We consider a lumped parameter system that exhibits only three mode of vibration: the torsion of the drive-train, the first mode of tower bending and flapping of blades. In general the system should be modelled as a complex distributed parameter system that exhibits many mode of vibration.
  - The blades move synchronously, meaning there are not distinguish between individual blade flapping. Furthermore we assume that the wind is uniformly distributed across the space, though in reality, each blade may experience varying forces due to fluctuations in wind speed.
- Wind:
  - The tower yaw control is not addressed under the assumption that the wind consistently approaches the blades head-on.
  - Not taken into account the tower shadow, which refers to the phenomenon where the tower obstructs the wind flow, causing localized modifications in its direction and intensity.

  - We omitted the consideration about the wind shear, which accounts for the cyclic variation in wind speed experienced by a blade due to the mean speed gradient - the increase in wind speed with height. Wind shear is particularly notable in two-bladed turbines.
  - We neglected the rotational sampling, which involves the cyclic aerodynamic forces experienced by the blades due to the non-uniform distribution of wind across space.

- Generator:

  - The generator is represented by his steady state model, since the dynamic of electrical quantities are much faster than the dynamic of the mechanical ones.
  - The nonlinear torque-speed diagram of the generator is approximated with a linear function, since it will work around the rated values of torque and speed, due to the implemented control strategy.
  - Only the third operational region of the wind turbine control profile is considered, which is the region where the wind speed is equal or greater than the rated value. This because the type of control we are going to implement is not used for speed below the rated one or above the cut-out speed, which defines the other operational regions.

- Aerodynamic:

  - The forces acting on the blades considered in the analysis are the thrust force (which is the force that push in direction of the wind the turbine) and the aerodynamic torque.
  - An analytical and differentiable function for the aerodynamic coefficients is introduced, while they are usually provided by blade manufactures in the form of look-up tables.

2.3 Mathematical model

In the following the several steps used to derive a mathematical model are illustrated.

2.3.1 Mechanical subsystem and pitch actuators

The mechanical subsystem includes both the mechanical dynamics of the blade (drive-train) and the tower. Starting from the Lagrange equations [1]:

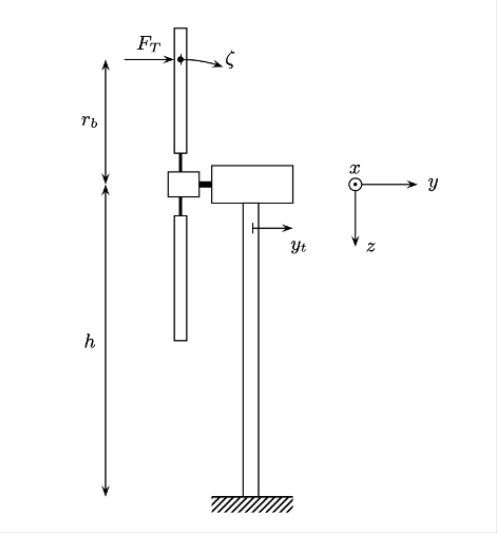

Figure 3: Schematic diagram of the mechanical subsystem

$$\frac{d}{dt}\left(\frac{\partial E_k}{\partial \dot{q}_i}\right) - \frac{\partial E_k}{\partial q_i} + \frac{\partial E_d}{\partial \dot{q}_i} + \frac{\partial E_p}{\partial q_i} = Q_i \tag{1}$$

where the the generalised coordinates are:

$$q = \begin{bmatrix} y_t & \zeta & \theta_r & \theta_g \end{bmatrix}^T \tag{2}$$

where y_t is the axial displacement of the nacelle, ζ is the angular displacement out of the plane of rotation and θ_r and θ_g are the angular positions of the rotor and generator, respectively. The kinetic, dissipated and potential energy are:

$$E_k = \frac{m_t}{2}\dot{y}_t^2 + \frac{N_b}{2}m_b(\dot{y}_t^2 + r_b\dot{\zeta})^2 + \frac{J_r}{2}\Omega_r^2 + \frac{J_g}{2}\Omega_g^2 \tag{3}$$

$$E_d = \frac{B_t}{2}\dot{y}_t^2 + \frac{N_b}{2}B_b(r_b\dot{\zeta})^2 + \frac{B_s}{2}(\Omega_r - \Omega_g)^2 \tag{4}$$

$$E_p = \frac{K_t}{2}\dot{y}_t^2 + \frac{N_b}{2}K_b(r_b\dot{\zeta})^2 + \frac{K_s}{2}(\theta_r - \theta_g)^2 \tag{5}$$

and the vector of generalized load is:

$$Q = \begin{bmatrix} NF_T & NF_T r_b & T_r & -T_g \end{bmatrix}^T \tag{6}$$

where F_T is the total trust force generated by the wind on the blades, T_r is the aerodynamic torque developed by the turbine, r_b is the distance from the axis of rotation where the lumped force F_t is applied and T_g is the electromagnetic torque of the generator. For the parameters, see the table in the Appendix.
Then replacing the equations (3),(4),(5) and (6) in the Lagrange's equation (1), we obtain the mechanical model:

$$\mathbf{M} = \begin{bmatrix} m_t + N_b m_b & N_b m_b r_b & 0 & 0 \\ N_b m_b r_b & N_b m_b r_b^2 & 0 & 0 \\ 0 & 0 & J_r & 0 \\ 0 & 0 & 0 & J_g \end{bmatrix} \tag{7}$$

$$\mathbf{C} = \begin{bmatrix} B_t & 0 & 0 & 0 \\ 0 & B_b r_b^2 & 0 & 0 \\ 0 & 0 & B_s & -B_s \\ 0 & 0 & -B_s & B_s \end{bmatrix} \tag{8}$$

$$\mathbf{K} = \begin{bmatrix} K_t & 0 & 0 & 0 \\ 0 & K_b r_b^2 & 0 & 0 \\ 0 & 0 & K_s & -K_s \\ 0 & 0 & K_s & -K_s \end{bmatrix} \tag{9}$$

$$\dot{x} = \begin{bmatrix} 0_4 & I_4 \\ -\mathbf{M}^{-1}\mathbf{K} & -\mathbf{M}^{-1}\mathbf{C} \end{bmatrix} x + \begin{bmatrix} 0_4 \\ \mathbf{M}^{-1} \end{bmatrix} Q \tag{10}$$

with the state x being defined as

$$x = \begin{bmatrix} q^T & \dot{q}^T \end{bmatrix}^T \tag{11}$$

Actually, the absolute angular positions of the drive-train components θ_r and θ_g are of no interest and moreover they may introduce numerical problems. So, it is convenient to remove them from the state and replace them with a single state variable $\theta_s = \theta_r - \theta_g$ denoting the torsion angle.
Moreover, we include in the system the pitch actuator dynamics:

$$\dot{\beta} = -\frac{1}{\tau}\beta + \frac{1}{\tau}\beta_d \tag{12}$$

where τ is the time constant of the pitch actuator, β is the pitch angle of the blades and the pitch angle reference β_d is the control input of the system.
Finally we get to the system in the following form: [1]:

$$\begin{cases} \dot{\tilde{x}} = A\tilde{x} + B\tilde{u} \\ \tilde{y} = C\tilde{x} \end{cases} \tag{13}$$

where the enlarged state, input and output vectors are:

$$\tilde{x} = \begin{bmatrix} y_t & \zeta & \theta_s & \dot{y}_t & \dot{\zeta} & \Omega_r & \Omega_g & \beta \end{bmatrix}^T \tag{14}$$

$$\tilde{u} = \begin{bmatrix} F_T & T_r & T_g & \beta_d \end{bmatrix}^T \tag{15}$$

$$\tilde{y} = \begin{bmatrix} \dot{y}_t & \dot{\zeta} & \Omega_r & \Omega_g \end{bmatrix}^T \tag{16}$$

and the matrices $\tilde{A}$, $\tilde{B}$ and $\tilde{C}$ are:

$$\tilde{A} = \begin{bmatrix} 0_3 & L_{3X4} & 0_{3X1} \\ -\mathbf{M}^{-1}\tilde{\mathbf{K}} & -\mathbf{M}^{-1}\mathbf{C} & 0_{4X1} \\ 0_{1X3} & 0_{1X4} & -\frac{1}{\tau} \end{bmatrix}, \quad \tilde{B} = \begin{bmatrix} 0_3 & 0_{3X1} \\ \mathbf{M}^{-1}\mathbf{Q} & 0_{4X1} \\ 0_{1X3} & \frac{1}{\tau} \end{bmatrix}, \quad \tilde{C} = \begin{bmatrix} 0_{4X3} & I_4 \end{bmatrix} \tag{17}$$

while the matrices A, B and C are:

$$A = \begin{bmatrix} 0_3 & L_{3X4} \\ -\mathbf{M}^{-1}\tilde{\mathbf{K}} & -\mathbf{M}^{-1}\mathbf{C} \end{bmatrix}, \quad B = \begin{bmatrix} 0_3 \\ \mathbf{M}^{-1}\mathbf{Q} \end{bmatrix}, \quad C = \begin{bmatrix} 0_{4X3} & I_4 \end{bmatrix} \tag{18}$$

with

$$L_{3X4} = \begin{bmatrix} 1 & 0 & 0 & 0 \\ 0 & 1 & 0 & 0 \\ 0 & 0 & 1 & -1 \end{bmatrix}, \quad \tilde{\mathbf{K}} = \begin{bmatrix} K_t & 0 & 0 \\ 0 & K_b r_b^2 & 0 \\ 0 & 0 & K_s \\ 0 & 0 & -K_s \end{bmatrix}, \quad \mathbf{Q} = \begin{bmatrix} N & 0 & 0 \\ N r_b & 0 & 0 \\ 0 & 1 & 0 \\ 0 & 0 & -1 \end{bmatrix} \tag{19}$$

2.3.2 Aerodynamic subsystem

The aerodynamic subsystem describe the interaction of the wind with the blades of the wind turbine. Commonly, thrust force and the aerodynamic torque are described in terms of non-dimensional thrust (C_T) and power coefficient (C_P) :

$$\begin{bmatrix} F_T \\ T_r \end{bmatrix} = \begin{bmatrix} \frac{\rho \pi R^2}{2} C_T(\frac{\Omega_r R}{V_e}, \beta) {V_e}^2 \\ \frac{\rho \pi R^3}{2} C_Q(\frac{\Omega_r R}{V_e}, \beta) {V_e}^2 \end{bmatrix} \tag{20}$$

Where V_e is defined as:

$$V_e = V - \dot{y}_t - r_b \dot{\zeta} \tag{21}$$

where V is the wind speed.
C_P characterizes the ability of the wind turbine to capture wind energy; Finding a good approximation of those coefficients is not trivial, and often empirical formulas are used. We choose to use these formulas [3][4]:

$$C_P = \left(\frac{\frac{116}{\lambda_i} - 0.4\beta - 5}{2} \right) e^{\frac{-21}{\lambda_i}} \tag{22}$$

$$C_T = \left(\frac{4a(1-a)(2a(1-a))}{\lambda^2} + 1 \right) \tag{23}$$

, where λ_i, a and λ are defined as:

$$\frac{1}{\lambda_i} = \frac{1}{\lambda + 0.08\beta} - \frac{0.035}{1 + \beta^3} \tag{24}$$

$$a = \frac{2}{3} \left(\cos \left(\frac{\arccos(\frac{27 C_P}{8} - 1) + 2\pi}{3} \right) + \frac{2}{3} \right) \tag{25}$$

$$\lambda = \frac{\Omega_r R}{V} \tag{26}$$

As we can see all these quantities are affected by the pitch angle.

2.3.3 Electrical subsystem

Finally, to transform the mechanical power generated by the movement of the blades, there is a power generation unit which can be represented by a static relationship:

$$T_g = B_g(\Omega_g - \Omega_s) \tag{27}$$

where B_g and Ω_s are two coefficients which depends on the generator characteristics.

3 Problem formulation

The control objective is to minimize the energy cost produced by wind turbines, which involves different values to be minimized. These costs are actually closely related and sometimes conflicting. Therefore, they should not be pursued separately. The partial goals we are going to address are energy capture, mechanical loads and actuator limitations.

- The maximization of the energy capture, taking into account safe operation restrictions. More precisely, we want to limit the generated power below the maximum value to avoid overloading, that would damage the electric generator. Also we want to keep the latter above a minimum value to verify that we are in the third control operational region.
- The minimization of the mechanical loads, that may cause fatigue damage on several devices, thereby reducing the useful life of the system. Since the overall cost of the WECS is therefore spread over a shorter period of time, the cost of energy will rise. In particular we take into account the dynamic loads induced by the temporal distribution of the wind speed profile. The latter comprise variations in the aerodynamic torque that propagate down the drive-train and variations in the aerodynamic loads that impact on the mechanical structure. Therefore the controller must provide damping at the vibration modes.
- Adding information about the constraints of the actuator dynamics in the controller logic. Omitting constraints during the controller operation can therefore deteriorate the control system stability. Moreover, we want to reduce the fatigue on the pitch actuator, therefore increasing its life time and decreasing its energy consumption.

The control strategy will be based on the pitch angle control, which consists in the rotation of the blades around their longitudinal axis. Through this kind of control we can shape the aerodynamic response in above the rated wind speeds. Thus, despite the wind fluctuations we will be able to keep the operating point of the wind turbine in the neighborhood of the rated power, while preserving the structural integrity of the system.

4 Nonlinear Model Predictive Control - NMPC

We decided to use a NMPC to solve our problem, which is a closed loop approach based on a nonlinear constrained optimization program. It consists in the iterative solution of a Finite Horizon Optimal Control Problem (FHOCP) at each sampling time, initializing the model at the current state value. The solution of the FHOCP is an optimal sequence of control inputs, but only the first element of this sequence is applied to the system, resulting in the reciding horizon strategy. At the next time step the optimization problem is solved again, after updating the initial state with current measure. Therefore, the NMPC is a closed-loop online control technique [5],[6] [7].

4.1 Numerical integration

In order to solve the optimization problems, we compute the trajectories of the system model through numerical integration, since analytical trajectories computation is generally

not possible. The system model was initially built in Simulink, in order to test the open-loop trajectories with the maximum accuracy. In fact, in Simulink we exploited the integration method ODE45 with variable step-size, which means that the latter is dynamically updated by the solver. The same model was built in Matlab exploiting forward Euler and ODE45, both with a fixed time step. The three different methods were compared, using several values of the sampling frequency over a open loop trajectory of $100s$:

Simulation Method	**Step Size**	**Time (s)**
Simulink Scheme	Variable (ODE45)	33.4080
Forward Euler	Fixed ($5ms$)	0.6788
ODE45	Fixed ($10ms$)	24.6725

Table 1: Simulation times for different integration methods

The integration method that gave the best trade-off between accuracy and computation efficiency was Forward Euler, and it was the one chosen to solve the optimization problems.

4.2 FHOCP

The considered FHOCP is a multi-objective optimization program and it is in the form:

$$\underset{\beta_d(1)\dots\beta_d(N)}{min} \sum_{i=1}^{N} (P_{rated}(i) - P_g(i))^T Q_1 (P_{rated}(i) - P_g(i)) + \dot{y}_t(i)^T Q_2 \dot{y}_t(i) + \dot{\beta}(i)^T R \dot{\beta}(i)) \quad (28)$$

s.t

$$\tilde{x}(i+1|i) = \tilde{f}(\tilde{x}(i), \tilde{u}(i)) \quad (29a)$$
$$\tilde{x}(0) = \tilde{x}_0 \quad (29b)$$
$$\beta_{min} \leq \beta(i) \leq \beta_{max} \quad (29c)$$
$$\dot{\beta}_{min} \leq \dot{\beta}(i) \leq \dot{\beta}_{max} \quad (29d)$$
$$y_{t,min} \leq y_t(i) \leq y_{t,max} \quad (29e)$$
$$P_{g,min} \leq P_g(i) \leq P_{g,max} \quad (29f)$$

4.2.1 Cost function

The cost function of the FHOCP mathematically expresses the control objectives. We aim to minimize the quadratic difference between the generator power P_g and a reference, that is the generator power rated value P_{rated}. Secondly, we want to keep as low as possible the tower mechanical oscillation, and this objective is expressed by the term related to $\dot{y}_t$. Finally, we would achieve the two objectives above, by the minimal usage of the pitch actuator, and this is expressed by the last term, weighting the pitch angle rate.

Q_1, Q_2 and R are diagonal matrices that consent to enforce a trade-off between the different objectives.

4.2.2 Constraints

The equality constraints (29a) and (29b) impose that the system trajectories must be computed through the system model, starting from the initial state.
The inequality constraint (29c) limits the pitch angle to its feasible working area, where the aerodynamic coefficient of the blades are well defined. The inequality constraint (29d) restricts the pitch angle rate between a maximum and a minimum value imposed by the pitch actuator.
The last two constraints are related to wind turbine safety operation region. In fact, constraint (29e) ensures that the generator power does not exceed its limit, ensuring safe operations for the generator. While (29f) ensures structural integrity and prevents excessive mechanical stress on the tower.

4.3 Optimization variables reduction

The NMPC is an online technique; therefore the chosen sampling time directly affects the elapsed time for optimization routine. In particular the time needed to solve the optimization program increases as the number of optimization variables becomes larger. The latter can be expressed as:

$$N = \frac{T_{end}}{T_s} \tag{30}$$

where T_{end} is the prediction horizon and T_s the sampling time.
Therefore as T_s decreases, the computational burden of the optimization program rises.

4.3.1 Downsampling

For the reason above, the downsampling of optimization variables was employed. This means to solve the optimization program with a frequency that is lower than the sampling frequency at which the system is integrated. Two different approaches will be used.
The first approach, called "pure" downsampling, consists in dividing the time horizon in equally spaced intervals where the optimization variable is held constant in each interval. This technique leads to huge improvement in terms of computational efficiency, as can be shown in section 5.
The second approach is named collocation. With the latter, the time horizon is again divided in equally spaced intervals, but the optimization variables are interpolated using piece-wise continuous polynomials, in our case cubic splines. The use of a third order polynomial is necessary since we need to interpolate between 2 values (a initial one, calculated in the previous iteration, and a final one, object of our optimization) and 2 derivatives values (we suppose that the derivative in the initial and final point is zero), so we have 4 conditions and the cubic spline has 4 parameters.
Substituting the previous conditions in the polynomial equation we obtain

$$f(t) = at^3 + bt^2 + ct + d \quad \Rightarrow \quad f(t) = -2(x_2 - x_1)t^3 + 3(x_2 - x_1)t^2 + x_1 \tag{31}$$

with x_2 the final value and x_1 the initial value of the interval (to simplify the equation, without loss of generality, we suppose an interval of length 1).
This solution solves the problem with "pure" downsampling without sacrificing the computation time.

4.4 Warm-starting

In the NMPC warm-starting is employed, by initializing the solver at each time step with the solution computed at the previous time step shifted by one control move, to which a terminal element is added.
In our case the vector used to initialize the solver at time t is:

$$\begin{bmatrix}\beta_d^*(1|t-1) & ... & \beta_d^*(N|t-1) & \beta_d^*(N|t-1)\end{bmatrix} \tag{32}$$

4.5 Optimization algorithm

The FHOCP we want to solve takes the form of a constrained nonlinear program. For this reason a sequential quadratic programming approach was applied. The latter prescribes to approximate the nonlinear program into a quadratic problem at each iteration of the optimization algorithm. In particular at each iteration an auxiliary QP is generated [8]:

$$\begin{aligned} \min_{p^k} \nabla_x f(x^k)^T p^k + \frac{1}{2} p^{kT} \nabla_x^2 \mathcal{L}(x^k, \lambda^k, \mu^k) p^k \\ s.t \quad \nabla_x g(x^k)^T p^k + g(x^k) = 0 \\ \nabla_x h(x^k)^T p^k + h(x^k) \geq 0 \end{aligned} \tag{33}$$

We can notice that the linear term is the gradient of the cost function f evaluated at the current iterate x^k. The quadratic term is the Hessian of the Lagrangian function $\mathcal{L}$ evaluated at the current iteration of the primal and dual variables. The nonlinear constraints were linearized in x^k. The solution of such a QP generates the search directions in the space of the primal and dual variables, that we can use to perform a line search method, in order to compute the next iterate [8]:

$$\begin{aligned} x^{k+1} &= x^k + t^k p^k \\ \lambda^{k+1} &= \lambda^k + t^k \Delta\lambda^k \\ \mu^{k+1} &= \mu^k + t^k \Delta\mu^k \end{aligned} \tag{34}$$

where t^k is the step length at the iteration k, which is a scalar positive value.
The scalar t^k can be found by solving at each iteration an unconstrained back-tracking line search algorithm with Armijo stopping condition on the l_1 merit function:

$$T_1(x) = f(x) + \sum_{i=1}^{p} \sigma_i |g_i(x)| + \sum_{i=1}^{q} \tau_i max(0, -h_i(x)) \tag{35}$$

In practice, in the Back Tracking algorithm t^k is initially set to a maximum value t^{max} and then it is reduced at each iteration by a factor $\beta_{ls} \in (0,1)$ until a sufficient decrease in the directional derivative of the merit function is achieved, namely

$$T_1(x^k + t^k p^k) \leq T_1(x^k) + t^k c_{ls} D(T_1(x^k), p^k), \quad c_{ls} \in (0,1) \tag{36}$$

To solve the auxiliary QP (33) the gradients of both constraints and cost function and the Hessian of the Lagrangian are needed. In order to compute numerically the gradient, the central finite difference method, with step size η_{sqp}, was chosen as it guarantees a good trade-off between accuracy and computational efficiency. To evaluate the Hessian, the BFGS method was employed. The latter is completely described in [8]. BFGS was chosen as optimization algorithm since the FHOCP that has to be solved contains both non-linear and linear constraints. For instance, the Gauss-Newton method was discarded because it required to have linear constraints only, to achieve the best performances.
The optimization algorithm features several stopping criterion:

- The SQP iterations exceed a fixed maximum number N^{max}.
- The directional derivative of the Lagrangian is smaller than the tolerance TOL_{∇}.
- The update Δx^k of the primal variables is smaller than the tolerance TOL_x.
- The update Δf^k of the cost function is smaller than the tolerance TOL_f.

If, after the algorithm has ended, the constraints are either feasible or not satisfied by a value smaller than TOL_{constr}, then the solution is considered a feasible point which can be a local minimizer.
Moreover an initial guess for the the optimization variables, called β_{d0} is needed.
The values of such hyperparameters are showed in the Appendix.

4.6 Practical implementation

The term related to the generated power, that is $(P_{rated} - P_g)$, in the cost function (28) is substituted with $(\Omega_{rated} - \Omega_g)$. In fact since a static model was utilized to represent the generator, we have that:

$$P_g = T_g \Omega_g \tag{37}$$

therefore there is only a scaling factor between P_g and Ω_g. Consequently even the constraints $P_{g,min}$ and $P_{g,max}$ were respectively substituted with $\Omega_{g,min}$ and $\Omega_{g,max}$.
The equality constraints (29a) and (29b) regarding system trajectories and initial state consistency are not explicitly indicated in the constraints, instead they are automatically satisfied by embedding the simulation of the system model in the computation of the cost and constraint functions.
Inequality constraints (29c) on β, were imposed on β_d, that is the optimization variable. This was possible since the pitch actuator is represented by a first order dynamics, which does not have overshoots.
Moreover the pratical implementation of the NMPC requires a prediction of the wind profile. Therefore we assumed to have an estimation of the latter to run the NMPC. The estimate is a low pass filtered of the wind profile affecting the system.
Furthermore, the initial state of the system is assumed to be known.

5 Simulations and results

5.1 Downsampling and collocation results

In this section we are going to compare different simulations over a 100 seconds trajectory exploiting different downsampling methods.
The first simulation is produced without applying any downsampling.
The second one is produced applying $K = 10$, where K is the factor by which the optimization variables are reduced.
The lastest simulations are produced respectively with $K = 100$ and $K = 100$ with collocation.
For clarity the results related to Ω_g are shown with respect T_g, since these quantities are statically related. Values of T_g and y_t closer respectively to the torque rated value $T_n = 43kNm$ and $0m$ are better.

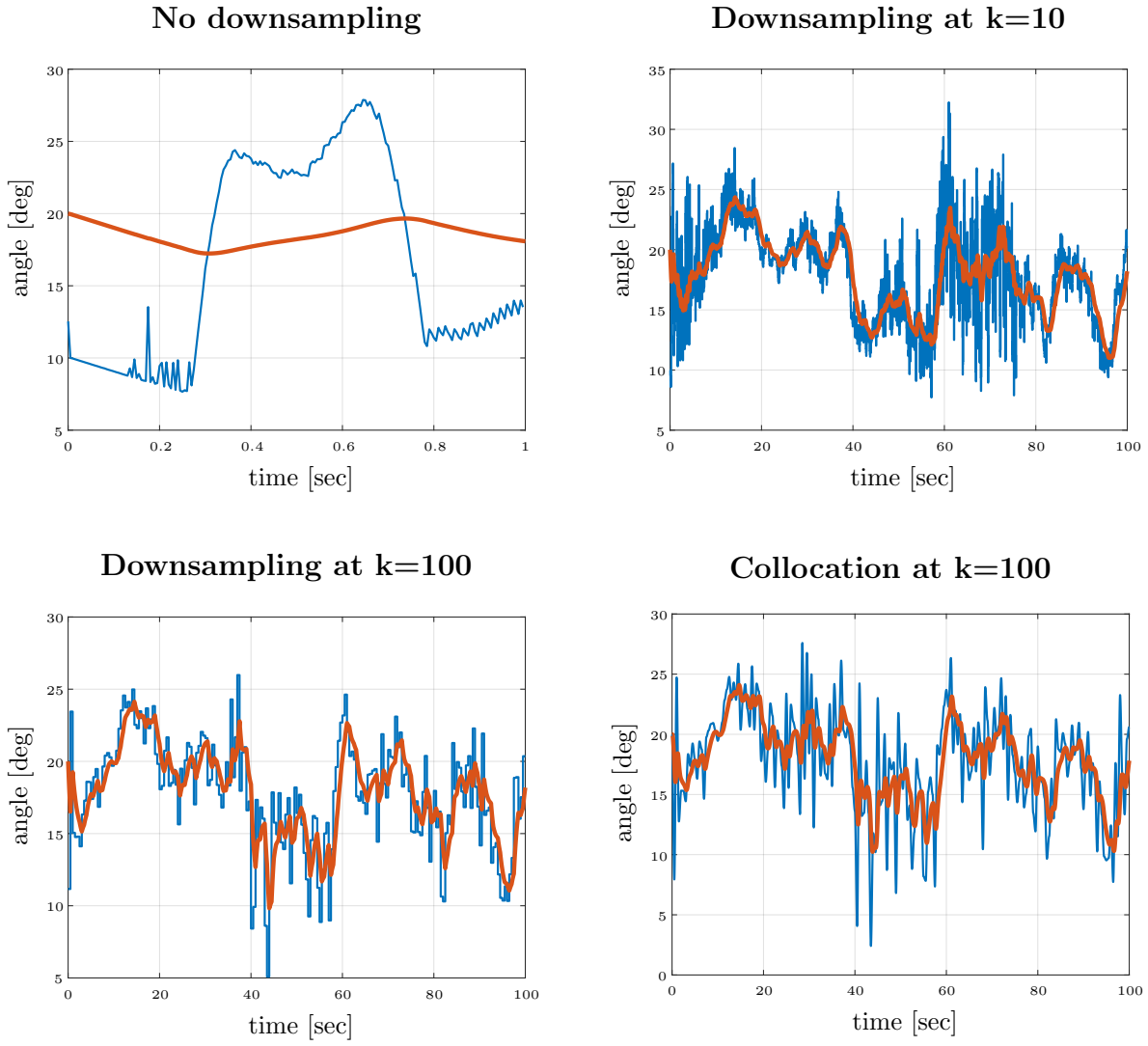

Figure 4: Comparison across multiple choices of downsampling on the pitch angle reference β_d (blue line) and the pitch angle β(red line)

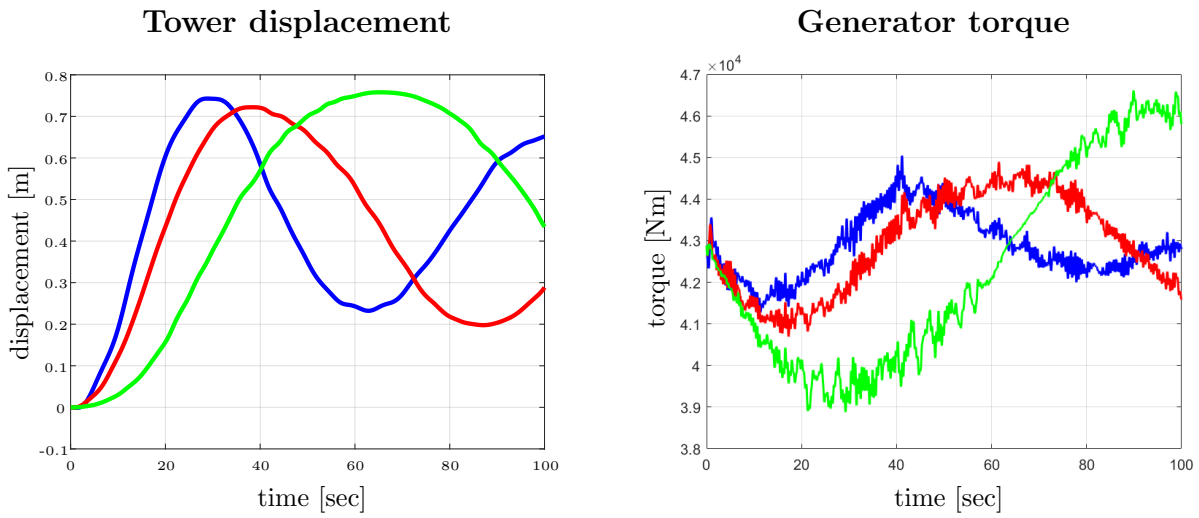

Figure 5: Comparison of the effect of different choices of downsampling: $K = 10$ (green), $K = 100$ (red) and collocation with $K = 100$ (blue)

As expected, stronger downsampling leads to a coarser control action and worse performances but better optimization time, as we can see in the next table.

Type of downsampling	K=1 (none)	K=10	K=100	K=100 and collocation
Time effort (s)	∼100000	3000	36	36

Table 2: Required time for simulating a $100s$ trajectory for different values of K

5.2 Ideal case VS real case

In this section we are going to compare the NMPC in two different cases. The ideal one, where both the NMPC and the model are simulated by applying the same wind profile; and the the real one, where the system is simulated by applying the real wind profile, while the NMPC is handled with an estimation of the wind profile.

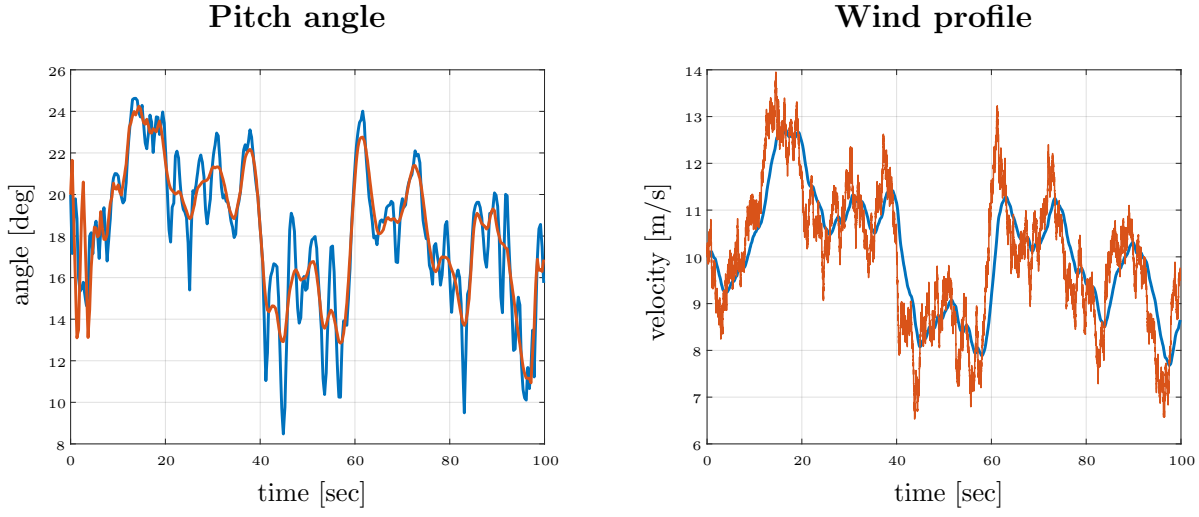

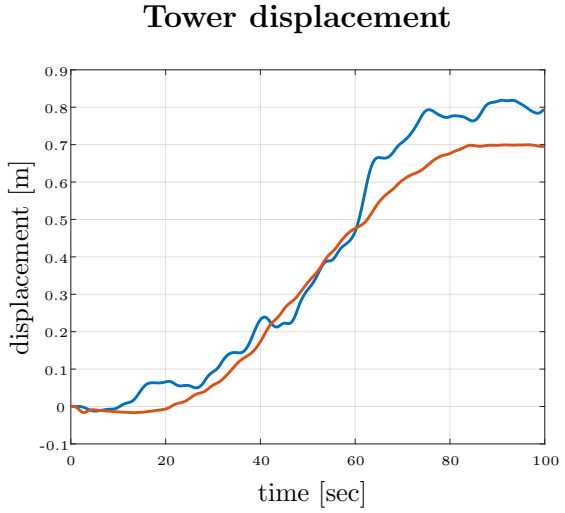

Figure 6: Comparison between the estimated wind case (blue line) and the ideal wind case (red line)

The results show that the NMPC is robust with the respect to poor wind estimation, however the y_t behaviour deteriorates.

5.3 Multi-objective optimization

In this section we are going to compare two different choices for the selection of the Q_1 and Q_2 matrices, that respectively weights Ω_g and $\dot{y}_t$. Here we propose a "torque focused" control, where the diagonal elements of Q_1 are 10000 times greater than the diagonal elements of Q_2, and a balanced control where the parameters of the two matrices are the same. R was set as a zero matrix.

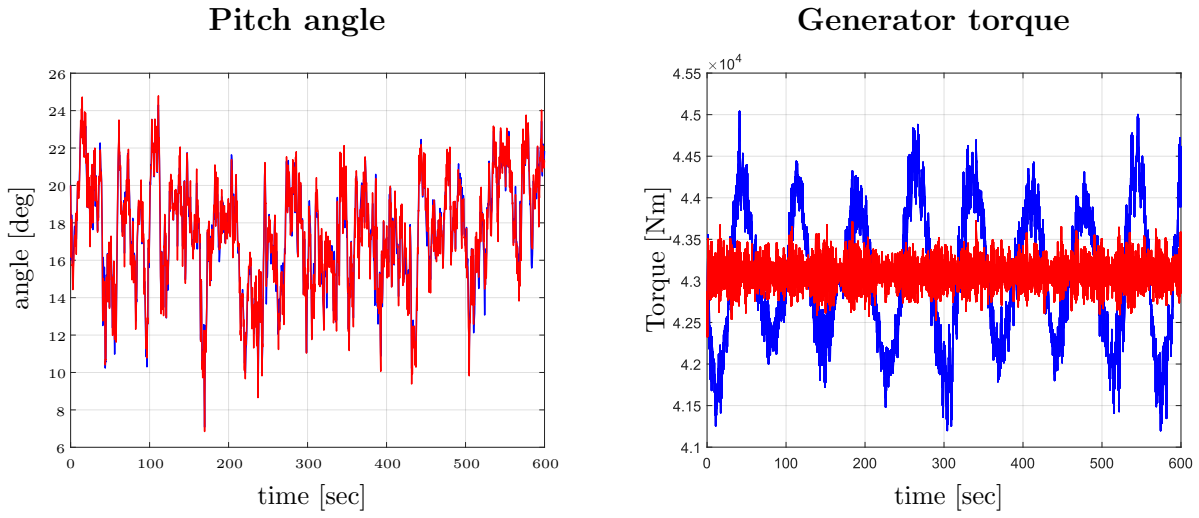

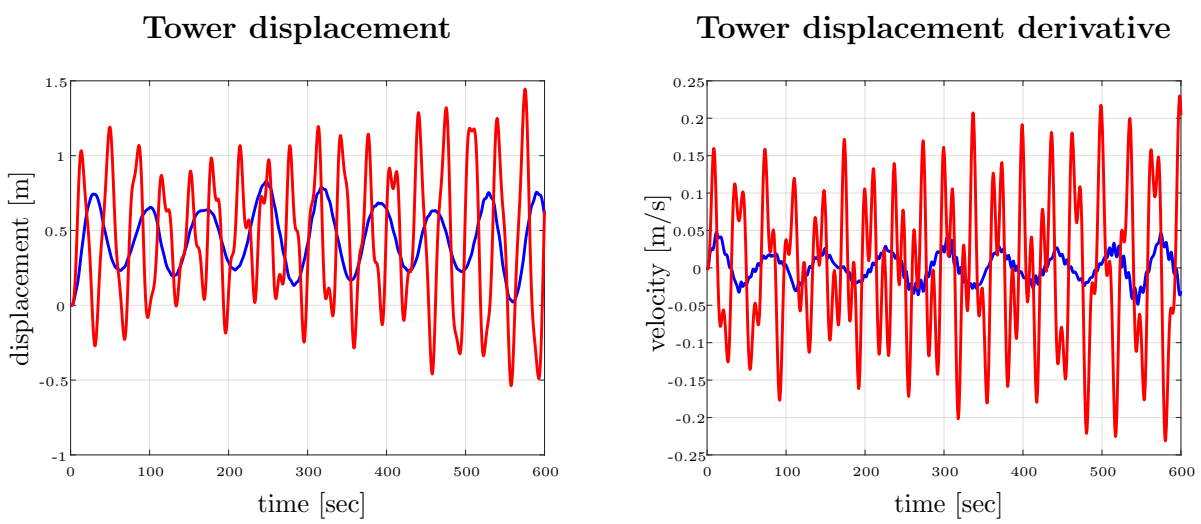

Figure 7: Comparison between the "torque focused" control (blue line) and the balanced control (red line)

As we can see the first control performs better on the torque but the tower displacement stabilization is poor (on the tower displacement derivative figure this is evident). An interesting fact is that, although the pitch trajectory angle of both controls is almost identical, the effects are widely different.

5.4 NMPC vs PID

Since the economical aspect of the controller implementation should be taken into account when choosing a suitable control strategy, in this section we analyze the performance of NMPC with more standard technique that requires less effort to be implemented, like a PID.

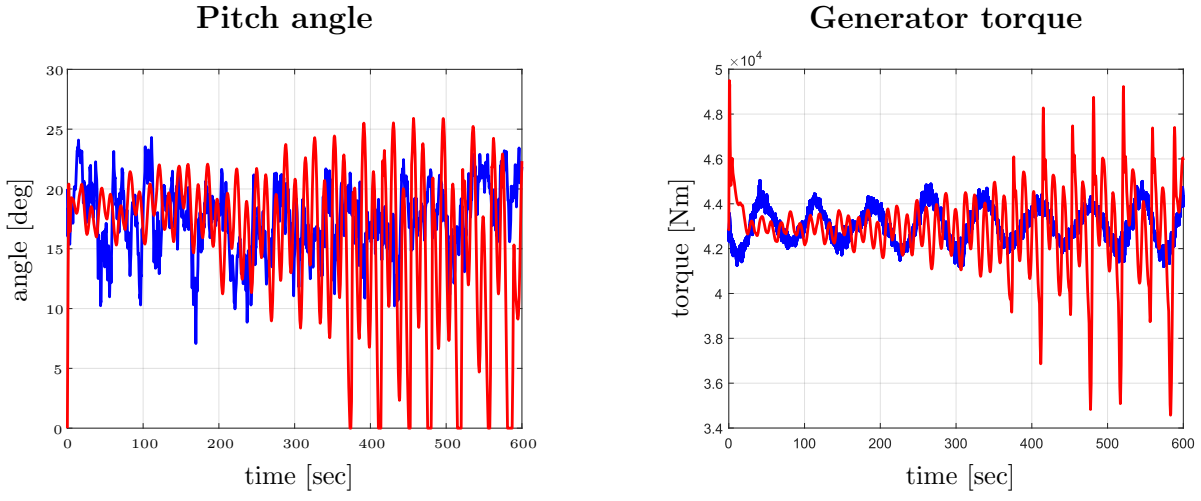

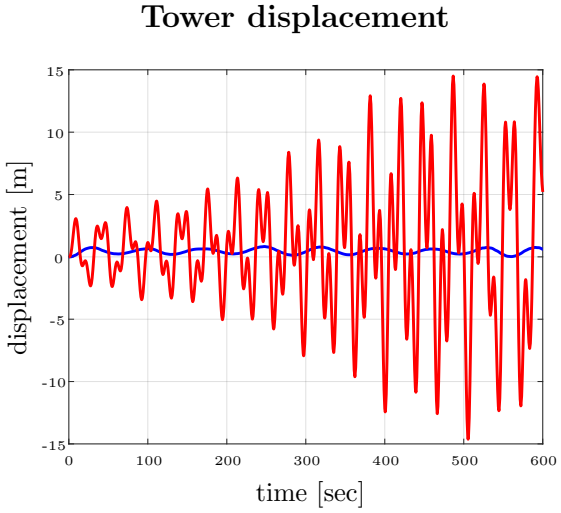

Figure 8: Comparison between the system response with the NMPC (blue line) and the system response with PID (red line)

As we can see, the performance of the system controlled with a PID regulator are not sufficient to guarantee the stability of the controlled system; in fact the tower oscillations are too large, leading to the failure of the system. It can be assessed that not only the NMPC is better, but is necessary to guarantee the stability of the wind turbine.

6 Appendices

6.1 Parameters tables

6.1.1 System parameters

Symbol	Parameter name	Parameter value	Unit
m_t	mass of the tower and nacelle	$347.460 \cdot 10^3$	kg
m_b	mass of each blade	$11 \cdot 10^3$	kg
r_b	point of application of ζ	30.75	m
J_r	inertia of the hub and rotor	$38.875152 \cdot 10^6$	kgm^2
J_g	inertia of the generator	$51.809 \cdot 10^3$	kgm^2
B_t	damping of the tower	2251.5	kg/s
B_b	damping of the blade	693.28	kg/s
B_s	damping of the transmission	$6.215 \cdot 10^6$	kgm/s
K_t	stiffness of the tower	$36.475 \cdot 10^3$	kg/s^2
K_b	stiffness of the blade	$47.916 \cdot 10^3$	kg/s^2
K_s	stiffness of the transmission	$867.637 \cdot 10^6$	kg/s^2
N_b	number of the blades	3	
τ	pitch actuators time constant	1	s
ρ	air density	1.293	$kg/(m^3)$
R	rotor radius	63	m
B_g	generator linear coefficient	$2 \cdot 10^5$	Nms/rad
Ω_s	synchronous speed	104.72	rad/s

Table 3: Symbol description

6.1.2 Optimization parameters

Parameter name	Parameter value
$y_{t,min}$	-5 m
$y_{t,max}$	+5 m
$\Omega_{g,min}$	-2.8 rad/s
$\Omega_{g,max}$	+2.8 rad/s
β_{min}	0°
β_{max}	45°
$\dot{\beta}_{min}$	-10 $degree/s$
$\dot{\beta}_{max}$	+10 $degree/s$

Table 4: FHOCP constraints

SQP		**Line Search**		**Tolerance**	
Parameter	Value	Parameter	Value	Parameter	Value
N^{max}	20	N_{ls}^{max}	20	TOL_x	10^{-12}
η_{sqp}	2^{-17}	βls	0.8	TOL_f	10^{-6}
γ	0.2	c_{ls}	0.05	TOL_∇	10^{-9}
β_{d0}	20°	t^{max}	1	TOL_{constr}	10^{-6}

Table 5: Hyperparameters of the optimization solver

Bibliography

[1] Hernán De Battista Fernando D. Bianchi and Ricardo J. Mantz. *Wind Turbine Control System*. 2007.

[2] W. Musial J. Jonkman S. Butterfield and G.Scott. *Definition of a 5-MW Reference Winnd Turbine for Offshore System Development*. 2009.

[3] S.I.Serma-Garcés Adriana Trejos and Cristian Guarnizo. "Overall Description of Wind Power System". In: *Ingenieria y Ciencia* (2014).

[4] Douglas Hunsaker. "Momentum Theory with Slipstream Rotation Applied to Wind Turbines". In: *Conference Paper* (2013).

[5] Nikola Hure. "Model Predictive Control of a Wind Turbine". In: ().

[6] Thorben Wintermeyer-Kallen Sebastian Dickler János Zierath Thomas Konrad Dirk Abel. "Weight-scheduling for linear time-variant model predictive wind turbine control toward field testing". In: *Forsch Ingenieurwes* (2021).

[7] Steffen Raach David Schlipf Frank Sandner Denis Matha1 and Po Wen Cheng. "Nonlinear Model Predictive Control of Floating Wind Turbines with Individual Pitch Control". In: *Proceedings of the American Control Conference* (2014).

[8] Lorenzo Fagiano. *Constrained Numerical Optimization for Estimation and Control*. 2023.